university of groningen

University Medical Center Groningen

University of Groningen

Charge transport and trap states in lead sulfide quantum dot field-effect transistors

Nugraha, Mohamad Insan

IMPORTANT NOTE: You are advised to consult the publisher's version (publisher's PDF) if you wish to cite from it. Please check the document version below.

Document Version
Publisher's PDF, also known as Version of record

Publication date:
2017

Link to publication in University of Groningen/UMCG research database

Citation for published version (APA):
Nugraha, M. I. (2017). *Charge transport and trap states in lead sulfide quantum dot field-effect transistors*. [Thesis fully internal (DIV), University of Groningen]. University of Groningen.

Copyright
Other than for strictly personal use, it is not permitted to download or to forward/distribute the text or part of it without the consent of the author(s) and/or copyright holder(s), unless the work is under an open content license (like Creative Commons).

The publication may also be distributed here under the terms of Article 25fa of the Dutch Copyright Act, indicated by the “Taverne” license. More information can be found on the University of Groningen website: https://www.rug.nl/library/open-access/self-archiving-pure/taverne-amendment.

Take-down policy
If you believe that this document breaches copyright please contact us providing details, and we will remove access to the work immediately and investigate your claim.

Downloaded from the University of Groningen/UMCG research database (Pure): http://www.rug.nl/research/portal. For technical reasons the number of authors shown on this cover page is limited to 10 maximum.

Download date: 29-04-2025

Chapter 5

Enabling Ambipolar to Heavy n-type Transport in PbS Quantum Dot Solids through Doping with Organic Molecules

This chapter discusses doping of PbS quantum dot (QD) films using benzyl viologen (BV) donor molecules. By engineering the energy level of the dopant and the PbS QDs through the use of particular capping ligands, the electrical characteristics of PbS QD field-effect transistors (FETs) can be tuned from ambipolar to strongly n-type. The doping significantly improves the charge carrier mobility by one order of magnitude to 0.64 $cm^2V^{-1}s^{-1}$ as revealed from four terminal conductivity measurements. In addition, the doping also reduces the contact resistance of the devices and assists the filling of carrier traps, which can explain the origin of the increased mobility.

M. I. Nugraha, S. Kumagai, S. Watanabe, M. Sytnyk, W. Heiss, M. A, Loi, J. Takeya, *ACS. Appl. Mater. Interfaces* **2017**, *Article ASAP*.

5.1 Introduction

PbS colloidal quantum dots (QDs) have been shown to be promising as semiconducting building blocks for optoelectronic devices, such as solar cells,[1–6] photodetectors,[7–10] and light-emitting devices.[11–13] This class of materials gives the possibility to fabricate electronic devices using solution processable methods such as blade-coating, dip-coating, printing, and roll-to-roll processes.[14–19] Recently, many efforts have been devoted to exploit PbS QDs as active material for field-effect transistors (FETs).[16,17,20,21] The fabrication of FETs offers the possibility to integrate them in more advanced electronic devices such as complementary metal oxide semiconductor (CMOS) devices - like inverters, integrated logic circuits, radio frequency identification (RFID) systems, etc.[22,23] Their use in FETs, however, is still challenging because they suffer from low charge carrier mobility due to the high number of carrier traps on their surface. Therefore, improving charge carrier mobility in FETs based on PbS QDs is crucial to enhance their potential for diverse applications.

Doping is an effective tool to improve charge carrier mobility in semiconductors.[23–26] Although PbS QDs are n-type on the basis of their stoichiometry,[4,21,27] many published studies show strategies to turn them into p-type semiconductors.[28,29] The p-type doping is mainly achieved by exposing samples to air, which gives rise to a significant increase of the hole mobility and density in the films.[28,29] A better control was achieved by evaporation of sulphur and selenium, or acting on the surface of the QDs with specific ligands.[4,21,30] On the other hand, studies on heavy n-type doping of PbS QD films are still limited. The energy offset often built at the interface of semiconductor and dopant is responsible for inefficient electron transfer from the HOMO of the dopant to the LUMO of the semiconductor.[31] Recently, benzyl viologen (BV) has been reported as a promising n-type dopant for the carbon nanotubes and MoS_2 systems.[25,32] Due to its shallow HOMO level, BV molecule treatment induces carrier doping in samples which favours electron transfer to the semiconducting films. To date, the use of BV as n-type dopant in PbS QD films has not been investigated yet. This leaves a question on the possibility to use BV for obtaining strong n-type doping of the PbS films and improving the performance of FET devices based on these QDs.

In this chapter, we report a strategy for doping PbS quantum dot solids using BV as the donor molecules. By combining the use of BV with engineering of the quantum dot energy levels through the use of several capping ligands, we are able to effectively tune the electrical properties of PbS QD-FETs from ambipolar to heavily n-type. With this BV treatment, we improved the electron mobility by one order of magnitude and we reduced the contact resistance down to 0.77 kΩcm. Furthermore, the four-terminal (4T) conductivity transistor measurements

confirmed the efficient doping of PbS QD films after BV treatment leading to electron mobility as high as 0.64 $cm^2V^{-1}s^{-1}$, the highest value reported for the low-temperature processed PbS QD-FETs employing SiO_2 as a gate dielectric.

5.2 Doping strategy using Benzyl Viologen (BV)

The successful doping of a semiconductor device is determined by the effective charge transfer from the dopant molecules to the semiconducting films or vice versa. Several methods have been used to introduce efficient doping of QD films including mixing a solution of dopants and QDs prior to film deposition, infiltrating a semi-metallic material into the active channels, and dipping the deposited semiconducting films into the dopant solution.[22,31,33,34] Among others, the dipping method has been shown to enable highly efficient optoelectronic devices fabricated with heavily-doped PbS QD films.[34] Furthermore, this method has also been used on a broad range of semiconductors leading to significant increase of the film conductivity in the fabricated transistors.[25,32,35–36]

To heavily dope the PbS QD films, we treated the semiconducting films with BV donor molecules, which have a redox potential of -0.79 V (BV^0/BV^+) relative to standard hydrogen electrode (SHE).[25,32] This redox potential corresponds to a HOMO level of -3.65 eV with respect to the vacuum level. Kiriya et al. reported that the BV molecules have a second redox potential after releasing an electron, which results in the BV^+ state.[25] In this state, the redox potential (BV^+/BV^{2+}) turns to -0.33 V relative to SHE, which corresponds to a HOMO level of -4.11 eV with respect to the vacuum level. The chemical structure of BV is shown in Figure 5.1 (a). In this study, doping of PbS films is done by dipping the deposited films into the BV solution for a specific time. The configuration of the BV-treated PbS QD-FETs is displayed in Figure 5.1 (b). To promote the transport of electrons from the dopant to the semiconductor, the LUMO level of the PbS films should be deeper than the HOMO level of the dopant. Recently, it has been reported that the HOMO/LUMO level of PbS QDs is strongly influenced by the cross-linking ligands.[37] Therefore, by varying the ligands, we are able to potentially tune the doping strength of the PbS QD films. Here, we use three kinds of ligands, namely 3-mercaptopropionic acid (3MPA), tetrabuthylammonium iodide (TBAI), and methylammonium iodide (MAI). The chemical structures of the ligands are shown in Figure 5.1 (a). These ligands have been reported to enable good performing FET devices based on PbS QDs.[12,14,28] By crosslinking PbS QDs with 3MPA ligands, the LUMO level of the materials is estimated to be around –3.6 and –3.7 eV, which are quite close to the HOMO level of BV.[37] With this energy level offset, some electrons are inefficiently transferred from BV to PbS films as shown in the schematics of Figure 5.1 (c). After releasing an electron, the BV^0 turns to BV^+ state which has HOMO of -4.11 eV. This HOMO value is significantly deeper than the

LUMO of 3MPA-capped PbS films, which blocks electron transfer from BV^+ to PbS, leading to an inefficient n-type doping of the PbS films after the BV layer deposition. This unfavourable energy offset could also explain the previously-reported inefficient n-type doping of lead chalcogenide films with cobaltocene.[31] With cobaltocene doping, the transport of charge carriers turns to n-type from ambipolar with a reduced current.

Other types of ligands, such as TBAI and MAI have been reported to result in a deep LUMO level for PbS QDs. The reported LUMO level using this class of ligands is as deep as −4.4 eV.[37] This LUMO level is importantly deeper than both the HOMO levels of BV^0 and of BV^+. Therefore, it opens the possibility to successfully obtain n-type doping in PbS QD films.

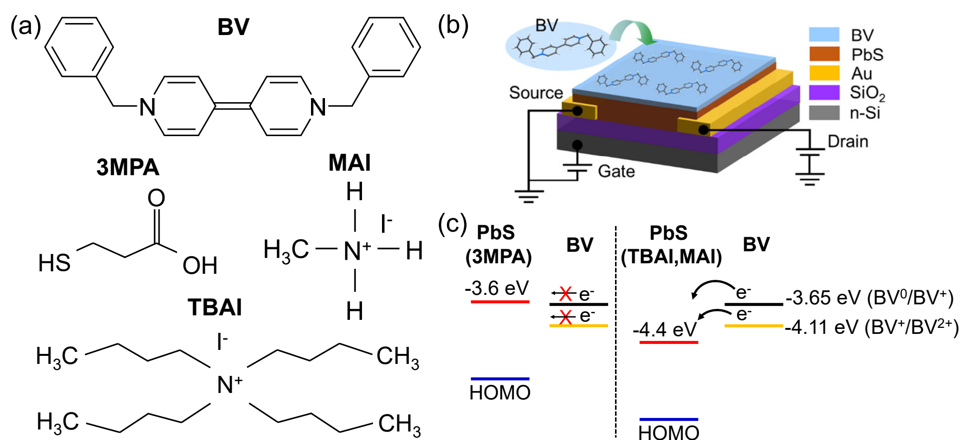

Figure 5.1 (a) Chemical structure of the BV molecules and the capping ligands used in this study; (b) device structure, and (c) schematic of the electron transfer mechanism from BV to PbS QDs with different capping ligands. After transferring an electron, BV^0 (black) turns to BV^+ state (orange) with deeper HOMO level.

5.3 Electrical characteristics of BV-doped PbS QD-FETs

The transfer characteristics of the pristine devices (before BV doping treatment) with different capping ligands are shown in Figure 5.2 (a)–(c). Obviously, the devices show ambipolar properties with more electron-dominated transport using all the three ligands. A pronounced difference is observed in the threshold voltages (V_{th}) of the devices. The devices with iodide ligands clearly show lower V_{th} than those with 3MPA ligands, which indicates a good passivation against carrier traps on the QD surfaces. The lower number of carrier traps in the PbS QD films with iodide ligands than those with 3MPA is also demonstrated by steeper transfer characteristics of the devices in the semi logarithmic scale as

displayed in Figure 5.2 (a)–(c). Meanwhile, in the p-channel characteristics, we also observe a slight hole current. However, in this study, we limit our analysis to the n-type transport because the hole current is much weaker than the electron current.

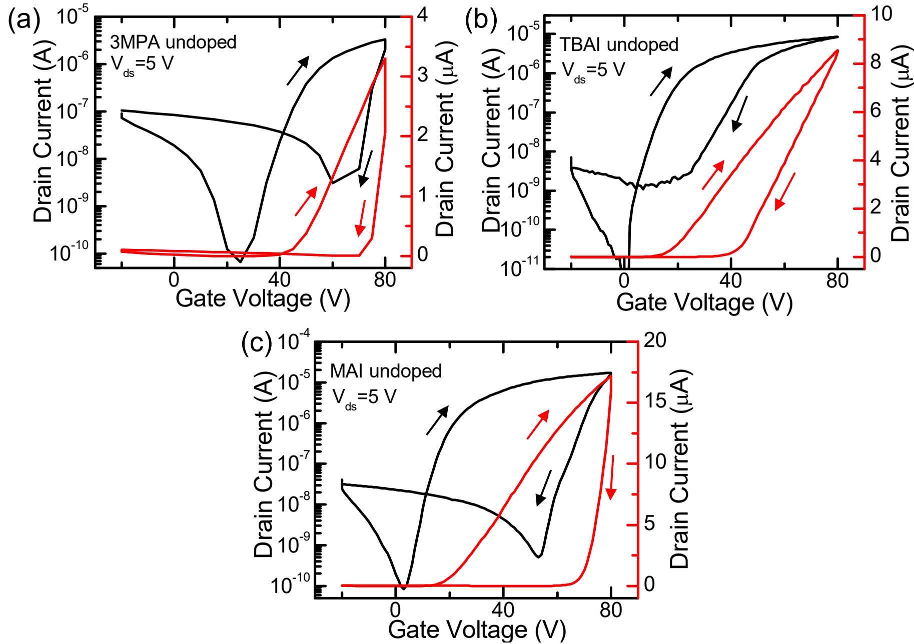

Figure 5.2 The transfer characteristics of the pristine devices with (a) 3MPA, (b) TBAI, and (c) MAI ligands.

TABLE 5.1 Electrical properties of PbS FETs with different capping ligands before and after BV treatment.

Ligands	2T Mobility ($cm^2V^{-1}s^{-1}$)		V_{th} (V)		Doping concentration (cm^{-2})
	Pristine	BV-treated	Pristine	BV-treated	
3MPA	2.6×10^{-3}	5.1×10^{-3}	36	18.8	1.6×10^{12}
TBAI	5.3×10^{-3}	1.4×10^{-2}	16.5	-17.1	3.2×10^{12}
MAI	0.03	0.32	12.2	-35	4.4×10^{12}

The extracted electron linear mobility, μ, in the pristine devices with different capping ligands is shown in Table 5.1. Obviously, the devices with MAI ligands show the highest μ among the other capping ligands, which is comparable to a previous report.[14] The lower μ in the devices with TBAI respect to the MAI

ones is attributed to the presence of remaining oleic acid ligands on the PbS QD surface which suppresses charge transport within the QD films. The remaining oleic acid is a result of the poor reactivity of TBAI in the ligand exchange process, due to non-acidity of the cation of TBAI ligands.[14]

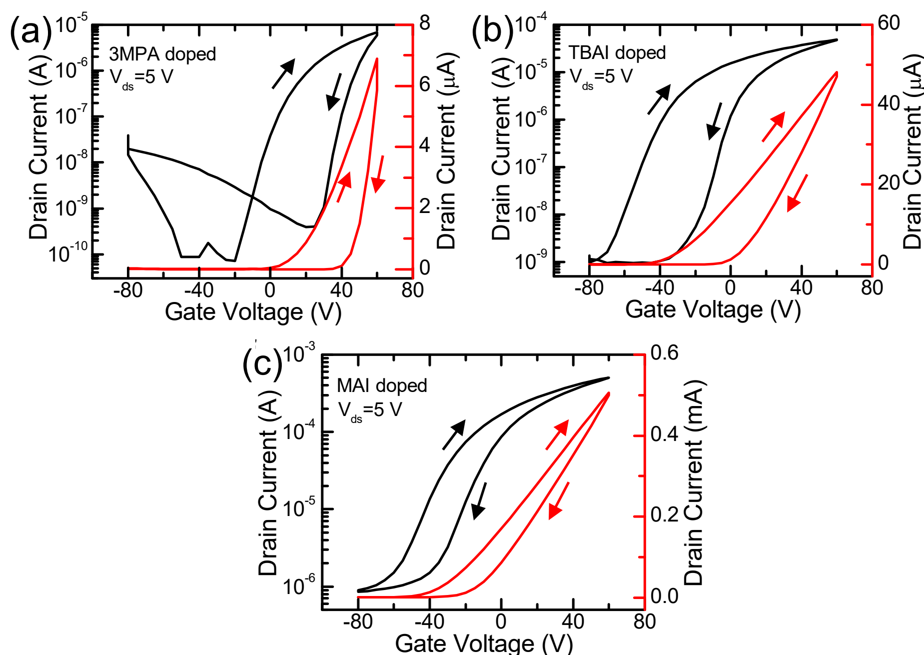

Figure 5.3 The transfer characteristics of the devices after BV doping treatment with (a) 3MPA, (b) TBAI, and (c) MAI ligands.

The transfer characteristics of the devices after BV treatment are shown in Figure 5.3 (a)–(c). In the devices with 3MPA ligands, we observe that the devices still show ambipolar characteristics with a slight increase of the source–drain current (I_{ds}) even after BV doping treatment, as shown in Figure 5.3 (a). The unaffected ambipolar properties are explained by our previous hypothesis that an unfavourable offset between the HOMO level of BV and the LUMO level of 3MPA-crosslinked PbS QDs leads to a blockade of the electron transfer from the BV layer to the PbS films. Nevertheless, some weak electron transfer from the BV^0 HOMO to the PbS LUMO may result in a shifting of the transfer characteristics to a negative direction, indicating the presence of a certain level of n-type doping. Instead, with TBAI and MAI ligands that enable the shift of the LUMO level of PbS QDs, we observe that the device characteristics turn to heavily n-type from ambipolar after BV doping treatment, as displayed in Figure 5.3 (b)–(c). In addition, the devices show a normally “on” operation as indicated by the transfer

characteristics in linear scale, which demonstrates the strong electron doping of the active material.

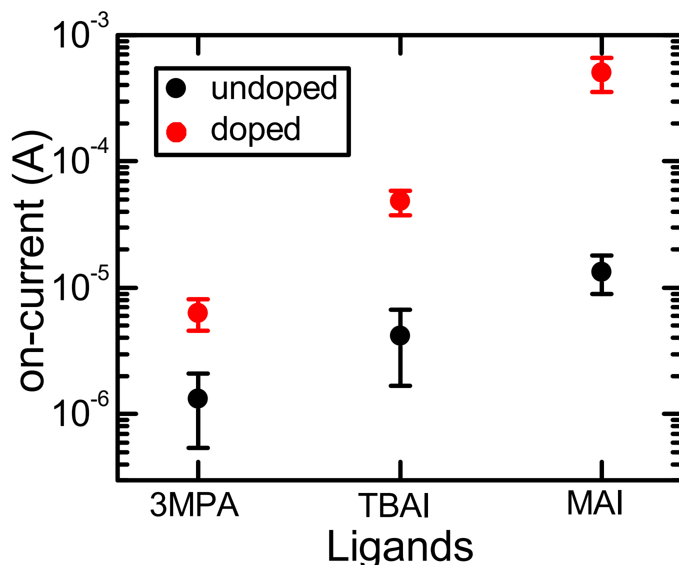

Figure 5.4 Comparison of on-current of the devices before and after BV doping treatment.

By analysing the transfer characteristics further, the devices with MAI ligands show the highest on-current after BV treatment among the other ligands as given in Figure 5.4. The on-current in the MAI-capped PbS FET devices is improved by more than one order of magnitude, whereas an improvement by only a factor of six is observed in the 3MPA-crosslinked devices after BV treatment. The extracted linear μ in all of the fabricated devices with different ligands before and after BV treatment is shown in Table 5.1. In the devices capped with 3MPA ligands, the μ is improved only by a factor of two. Importantly, a significant improvement in the μ (the maximum μ is 0.45 $cm^2V^{-1}s^{-1}$; the average μ is 0.32 $cm^2V^{-1}s^{-1}$) is observed in the devices with MAI ligands after treatment with BV, indicating a more efficient doping with respect to the case of PbS decorated by the other ligands. The devices with TBAI, which are suggested to have a doping mechanism similar to that of MAI, have a lower increase of the μ than that of the devices with MAI. This result can be associated to the more effective removal of oleic acid ligands with MAI than that with TBAI due to the acidity of the methylammonium cation.[15] In addition, among the other ligands, we observe that the BV doping treatment reduces the bias stress in devices with MAI ligands. This result is supported by the smaller hysteresis observed in devices with MAI after BV treatment with respect to the ones treated with the other ligands, as

shown in Figure 5.3 (c). Therefore, the proper choice of ligands combined with the use of BV results in n-type doping and more stable PbS QD transistors.

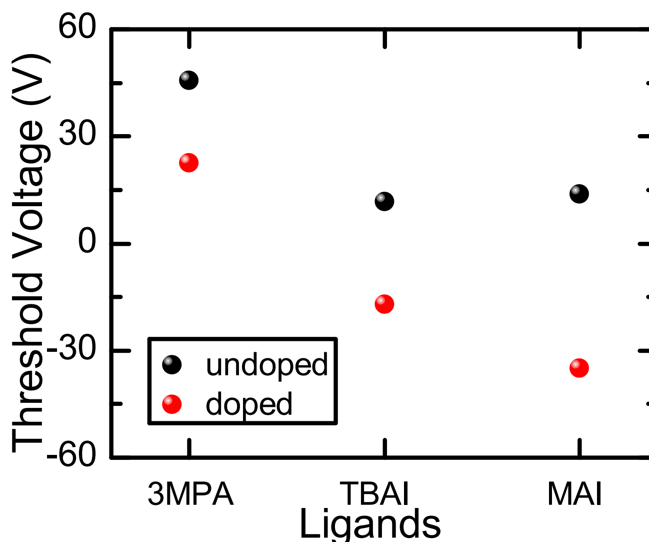

Figure 5.5 Threshold voltages of the devices before and after BV doping treatment.

We are then interested in estimating the doping concentration in devices after BV treatment. The doping concentration in FETs can be calculated by measuring the difference in V_{th} before and after doping ($n_{doping}=C_i\Delta V_{th}/e$) using equation (1.6). The V_{th} values of the devices with different capping ligands are given in Table 5.1. All devices show n-type doping, indicated by the shifting of V_{th} into the negative direction as is displayed in Figure 5.5. The doping concentration in all fabricated devices is shown in Table 5.1. The highest doping concentration is achieved in the devices with MAI ligands after BV treatment and is estimated to be about 4.4×10^{12} cm^{-2}, which is comparable to the accumulated charge carriers induced by the gate voltage (4.3×10^{12} cm^{-2} at V_g = 60 V). This high doping concentration can be the origin of the significant increase of the electron mobility in the devices with MAI, as it allows a more efficient filling of carrier traps. It is also worth noting that the doping concentration in the TBAI-capped devices is quite close to the one obtained in the MAI-capped devices. However, the degree of mobility improvement is remarkably different: in the MAI-capped devices, the μ is higher by one order of magnitude after BV doping treatment, whereas it is only a factor of two in the TBAI-capped devices. Although the doping concentration is quite close in the devices with both iodide ligands after BV treatment, some remaining oleic acid ligands on the PbS surfaces due to the incomplete removal of the native oleic acids with TBAI ligands might supress the charge transport between neighbouring QDs, as previously suggested.[14]

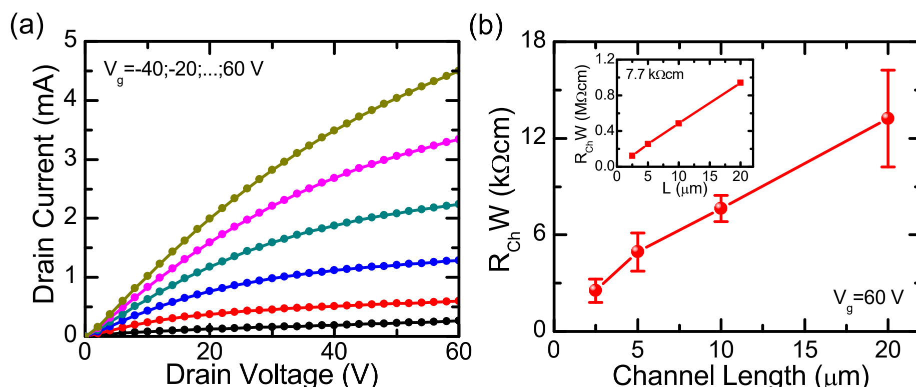

Figure 5.6 (a) Output characteristics and (b) channel resistances of the BV-doped devices. The inset shows the channel resistances of the pristine devices.

At this point, it is also interesting to measure the contact resistance (R_c) of the devices after BV treatment. Since the devices with MAI ligands show the most efficient n-type doping, we choose these systems for our next investigation. At a first sight, we did not observe a contact-limited transport in the output characteristics of the devices at low V_{ds} as shown in Figure 5.6 (a), suggesting low R_c in these devices. To estimate R_c, we fabricated FET devices to apply transmission-line method (TLM) with channel lengths of 2.5, 5, 10 and 20 μm. The measured channel resistance dependent on the channel length is shown in Figure 5.6 (b). The R_c is estimated from the intercept of the curve at the y-axis (zero channel length). With the BV doping treatment, the extracted contact resistance (normalized by W; R_cW) of the devices is 0.77 kΩcm, one order of magnitude lower than in the pristine devices as displayed in the inset of Figure 5.6 (b). This low R_c can also have a great impact on the improvement of the charge carrier mobility in the devices. It is expected that further improvement of the charge carrier mobility can be achieved by reducing the contact resistance; for instance, by the use of other metals with shallow work function, for the fabrication of source and drain electrodes.

5.4 4-terminal conductivity of BV-doped PbS QD-FETs

We then performed 4-terminal conductivity measurements to investigate the charge carrier mobility, μ in our devices. With these measurements, we are able to exclude the effect of contact resistance, which can limit the charge transport in the PbS FETs. The configuration of the devices for 4-terminal conductivity measurements is displayed in Figure 5.7 (a). In order to measure the 4-terminal voltage properly, we performed laser-etching treatment on the PbS films as

displayed in the schematic of Figure 5.7 (a). *L* and *W* of the 4-terminal transistor are 150 μm and 30 μm, respectively.

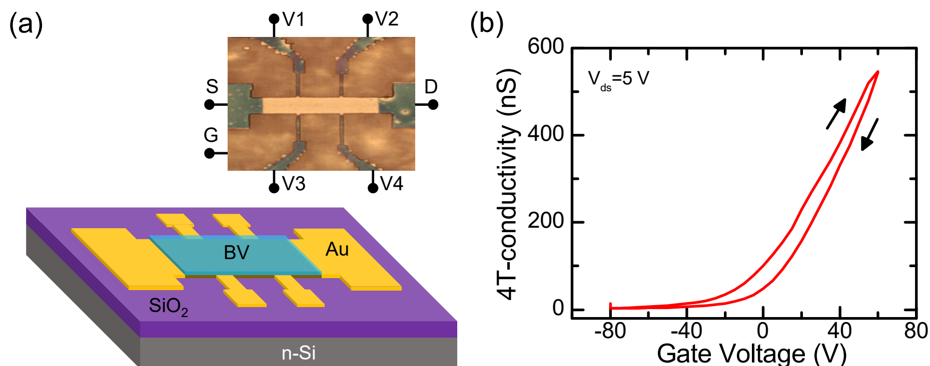

Figure 5.7 (a) Device configuration for 4T conductivity measurements. (b) 4T conductivity characteristics of BV-doped devices.

The 4-terminal conductivity in the devices is displayed in Figure 5.7 (b) and the mobility (μ_{4T}) is calculated using the equation,

$$\mu_{4T} = \frac{1}{C_i} \frac{\partial \sigma_{4T}}{\partial V_g} \tag{5.1}$$

where σ_{4T} is the 4-terminal conductivity. The maximum μ_{4T} among the devices with MAI ligands after BV doping is 0.64 $cm^2V^{-1}s^{-1}$ (the average mobility = 0.58 $cm^2V^{-1}s^{-1}$). To our knowledge, this value is the highest among the electron mobility reported so far in PbS QD-FETs with SiO_2 gate dielectric. Moreover, the high mobility after the BV treatment can be further improved by optimizing the interface quality of the PbS semiconducting films and the gate dielectric, for instance by using hydroxyl-free dielectrics, as in our previous report, opening great opportunities for the fabrication of highly performing solution processable electronic devices with PbS QDs.[16,39]

5.5 Conclusion

We have demonstrated n-type doping of PbS QD-FETs with the use of electron-donating BV molecules. By engineering the LUMO level of PbS semiconducting films through the use of different capping ligands, we successfully controlled the electrical characteristics of the PbS QD-FETs from ambipolar to heavily n-type. In the devices with MAI ligands, we observed a significant improvement of the electron mobility by more than one order of magnitude after the BV doping treatment. This high mobility is associated with an effective filling of carrier traps and a reduced contact resistance of the devices. The 4-terminal

conductivity transistor measurements revealed mobility as high as 0.64 $cm^2V^{-1}s^{-1}$ in the devices after BV treatment. These doping results open great opportunities for the exploitation of PbS QDs as n-type materials for broad electronic and optoelectronic applications.

5.6 Methods

Material preparation. PbS colloidal quantum dots of 3.6 nm in diameter were synthesized following a previously reported method.[39,40] For ligand exchange, we used three kinds of molecules, namely 3-mercaptopropionic acid (3MPA), tetrabuthylammonium iodide (TBAI), and methylammonium iodide (MAI). 3MPA ligand solution was prepared by dissolving 3MPA in methanol (115 mM). TBAI and MAI powders were dissolved in methanol (30 mM) to form TBAI and MAI ligand solution, respectively. The solutions were then filtered by PTFE filter (0.45 μm) before use.

The benzyl viologen (BV) solution was prepared according to previous reports with some modifications for the use in glove box.[25,32] 51 mg (0.12 mmol) of 1,1-dibenzyl-4,4-bipyridinium dichloride hydrate (TCI) was dissolved in distilled water (4.5 mL) inside a vial. Toluene (9.0 mL) was carefully layered on the aqueous layer, and 97 mg (2.5 mmol) of $NaBH_4$ was added into the bilayer system. The colourless aqueous layer immediately started to turn into deep violet with a generation of hydrogen gas. After 12 hours, the aqueous layer turned to colourless, and the top toluene layer became yellow. The toluene layer was separated and dried over $MgSO_4$, and filtered into a glass Schlenck flask. The solvent was removed under vacuum and heating, and then dry hexane/toluene (1:1 (v/v); 32 mL) was added into the yellow oily residue, affording a yellow solution. The BV solution was transferred into a glove box after argon bubbling for 15 minutes.

Device fabrication. We used SiO_2/n-Si substrates with lithographically-defined pre-patterned interdigitated Au electrodes. The thickness of the SiO_2 dielectric was 230 nm. The channel length and width of the devices were 20 μm and 1 cm, respectively. Before use, the substrates were cleaned with acetone and isopropanol using ultrasonicator for 10 min. The substrates were then dried at 120^oC for 10 min to remove residual organic solvents.

On the clean substrates, PbS films were then deposited by spin-coating the oleic acid-stabilized PbS solution in chloroform (10 mg/mL). To improve the conductivity of the films, the long oleic acid ligands were replaced by shorter molecules or halide atoms. The deposition of semiconducting thin film and ligand exchange (LE) were performed using layer-by-layer (LbL) for seven times to ensure complete LE process. For the LE, the ligand solution was dropped onto the previously-deposited oleic-acid capped PbS films for 30 s and then spin-casted for

60 s. After each LE process, pure methanol was dropped for another 30 s and then spin-casted for 60 s to remove native oleic acid ligands. The devices were then annealed at 120°C for 20 min to remove residual solvents and to enhance coupling between quantum dots. The BV doping treatment was done by dipping the previously-fabricated devices into BV solution for 3 minutes. The samples were then dried at room temperature under argon atmosphere. All device fabrication was done in glove box.

For the fabrication of 4-terminal (4T) FETs, we used bare SiO_2/n-Si substrates. Before use, the substrates were cleaned following the cleaning procedure mentioned above. As source-drain electrode, thermally-grown bottom contact Au (30 nm) with Cr (10 nm) as buffer layer was patterned using 4T transistor shadow mask. The deposition of PbS semiconducting thin films, ligand exchange, and BV doping treatment were done following the previously mentioned procedures.

Electrical measurement. The electrical characteristics of the fabricated devices were measured using an Agilent B1500A semiconductor parameter analyser connected to a probe station in a glove box.

5.7 References

[1] C. Piliego, L. Protesescu, S. Z. Bisri, M. V. Kovalenko, M. A. Loi, *Energy Environ. Sci.* **2013**, *6*, 3054.
[2] C. M. Chuang, P. R. Brown, V. Bulović, M. G. Bawendi, *Nat. Mater.* **2014**, *13*, 796.
[3] A. H. Ip, S. M. Thon, S. Hoogland, O. Voznyy, D. Zhitomirsky, R. Debnath, L. Levina, L. R. Rollny, G. H. Carey, A. Fischer, K. W. Kemp, I. J. Kramer, Z. Ning, A. J. Labelle, K. W. Chou, A. Amassian, E. H. Sargent, *Nat. Nanotechnol.* **2012**, *7*, 577.
[4] S. J. Oh, N. E. Berry, J.-H. Choi, E. A. Gaulding, T. Paik, S.-H. Hong, C. B. Murray, C. R. Kagan, *ACS Nano* **2013**, *7*, 2413.
[5] S. J. Oh, D. B. Straus, T. Zhao, J.-H. Choi, S.-W. Lee, E. A. Gaulding, C. B. Murray, C. R. Kagan, *Chem. Commun.* **2017**, 728.
[6] T. Zhao, E. D. Goodwin, J. Guo, H. Wang, B. T. Diroll, C. B. Murray, C. R. Kagan, *ACS Nano* **2016**, *10*, 9267.
[7] M. V Kovalenko, R. D. Schaller, D. Jarzab, M. A. Loi, D. V Talapin, *J. Am. Chem. Soc.* **2012**, *134*, 2457.
[8] S. Pichler, T. Rauch, R. Seyrkammer, M. Böberl, S. F. Tedde, J. Fürst, M. V. Kovalenko, U. Lemmer, O. Hayden, W. Heiss, *Appl. Phys. Lett.* **2011**, *98*, 53304.
[9] V. Sukhovatkin, S. Hinds, L. Brzozowski, E. H. Sargent, *Science* **2009**, *324*, 1542.
[10] K. Szendrei, F. Cordella, M. V. Kovalenko, M. Böberl, G. Hesser, M. Yarema, D. Jarzab, O. V. Mikhnenko, A. Gocalinska, M. Saba, F. Quochi, A. Mura, G. Bongiovanni, P. W. M. Blom, W. Heiss, M. A. Loi, *Adv. Mater.* **2009**, *21*, 683.
[11] M. A. Loi, C. Rost-Bietsch, M. Murgia, S. Karg, W. Riess, M. Muccini, *Adv. Funct. Mater.* **2006**, *16*, 41.
[12] J. Schornbaum, Y. Zakharko, M. Held, S. Thiemann, F. Gannott, J. Zaumseil, *Nano Lett.* **2015**, *15*, 1822.
[13] L. Sun, J. J. Choi, D. Stachnik, A. C. Bartnik, B.-R. Hyun, G. G. Malliaras, T. Hanrath, F. W. Wise, *Nat. Nanotechnol.* **2012**, *7*, 369.
[14] D. M. Balazs, D. N. Dirin, H.-H. Fang, L. Protesescu, G. H. ten Brink, B. J. Kooi, M. V. Kovalenko, M. A. Loi, *ACS Nano* **2015**, *9*, 11951.
[15] C. R. Kagan, E. Lifshitz, E. H. Sargent, D. V. Talapin, *Science.* **2016**, *353*, aac5523.
[16] M. I. Nugraha, R. Häusermann, S. Z. Bisri, H. Matsui, M. Sytnyk, W. Heiss, J. Takeya, M. A. Loi, *Adv. Mater.* **2015**, *27*, 2107.
[17] T. P. Osedach, N. Zhao, T. L. Andrew, P. R. Brown, D. D. Wanger, D. B. Strasfeld, L. Y. Chang, M. G. Bawendi, V. Bulović, *ACS Nano* **2012**, *6*, 3121.
[18] E. H. Sargent, *Nat. Photonics* **2012**, *6*, 133.
[19] J. Yang, M. K. Choi, D.-H. Kim, T. Hyeon, *Adv. Mater.* **2016**, *28*, 1176.
[20] W. Koh, S. R. Saudari, A. T. Fafarman, C. R. Kagan, C. B. Murray, *Nano Lett.* **2011**, *11*, 4764.
[21] S. J. Oh, N. E. Berry, J.-H. Choi, E. A. Gaulding, H. Lin, T. Paik, B. T. Diroll, S. Muramoto, C. B. Murray, C. R. Kagan, *Nano Lett.* **2014**, *14*, 1559.
[22] F. S. Stinner, Y. Lai, D. B. Straus, B. T. Diroll, D. K. Kim, C. B. Murray, C. R. Kagan, *Nano Lett.* **2015**, *15*, 7155.
[23] D. V Talapin, J.-S. Lee, M. V Kovalenko, E. V Shevchenko, *Chem. Rev.* **2010**, *110*, 389.
[24] D. V Talapin, C. B. Murray, *Science* **2005**, *310*, 86.
[25] D. Kiriya, M. Tosun, P. Zhao, J. S. Kang, A. Javey, *J. Am. Chem. Soc.* **2014**, *136*, 7853.

[26] J. Jang, W. Liu, J. S. Son, D. V Talapin, *Nano Lett.* **2014**, *14*, 653.
[27] Z. Ning, O. Voznyy, J. Pan, S. Hoogland, V. Adinolfi, J. Xu, M. Li, A. R. Kirmani, J. Sun, J. Minor, K. W. Kemp, H. Dong, L. Rollny, A. Labelle, G. Carey, B. Sutherland, I. Hill, A. Amassian, H. Liu, J. Tang, O. M. Bakr, E. H. Sargent, *Nat. Mater.* **2014**, *13*, 822.
[28] D. M. Balazs, M. I. Nugraha, S. Z. Bisri, M. Sytnyk, W. Heiss, M. A. Loi, *Appl. Phys. Lett.* **2014**, *104*, 112104.
[29] E. J. D. Klem, H. Shukla, S. Hinds, D. D. MacNeil, L. Levina, E. H. Sargent, *Appl. Phys. Lett.* **2008**, *92*, 212105.
[30] D. M. Balazs, K. I. Bijlsma, H.-H. Fang, D. N. Dirin, M. Dobeli, M. V. Kovalenko, M. A. Loi, *submitted.*
[31] W. Koh, A. Y. Koposov, J. T. Stewart, B. N. Pal, I. Robel, J. M. Pietryga, V. I. Klimov, *Sci. Rep.* **2013**, *3*, 2004.
[32] S. M. Kim, J. H. Jang, K. K. Kim, H. K. Park, J. J. Bae, W. J. Yu, I. H. Lee, G. Kim, D. D. Loc, U. J. Kim, E.-H. Lee, H.-J. Shin, J.-Y. Choi, Y. H. Lee, *J. Am. Chem. Soc.* **2009**, *131*, 327.
[33] D. K. Kim, Y. Lai, B. T. Diroll, C. B. Murray, C. R. Kagan, *Nat. Commun.* **2012**, *3*, 1216.
[34] A. R. Kirmani, A. Kiani, M. M. Said, O. Voznyy, N. Wehbe, G. Walters, S. Barlow, E. H. Sargent, S. R. Marder, A. Amassian, *ACS Energy Lett.* **2016**, 922.
[35] I. D. V. Ingram, D. J. Tate, A. V. S. Parry, R. Sebastian Sprick, M. L. Turner, *Appl. Phys. Lett.* **2014**, *104*, 153304.
[36] B. Lüssem, M. L. Tietze, H. Kleemann, C. Hoßbach, J. W. Bartha, A. Zakhidov, K. Leo, *Nat. Commun.* **2013**, *4*, 153506.
[37] P. R. Brown, D. Kim, R. R. Lunt, N. Zhao, M. G. Bawendi, J. C. Grossman, V. Bulovic, *ACS Nano* **2014**, *8*, 5863.
[38] A. G. Shulga, L. Piveteau, S. Z. Bisri, M. V. Kovalenko, M. A. Loi, *Adv. Electron. Mater.* **2016**, *2*, 1500467.
[39] L. Cademartiri, J. Bertolotti, R. Sapienza, D. S. Wiersma, G. von Freymann, G. A. Ozin, *J. Phys. Chem. B* **2006**, *110*, 671.
[40] M. A. Hines, G. D. Scholes, *Adv. Mater.* **2003**, *15*, 1844.